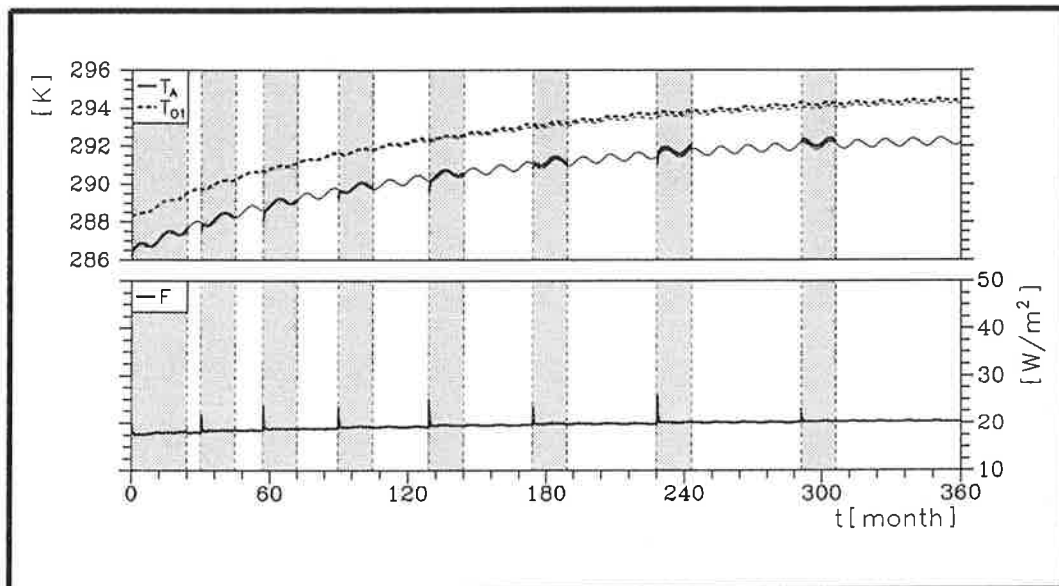




# Max-Planck-Institut für Meteorologie

## REPORT No. 169



### TECHNIQUES FOR ASYNCHRONOUS AND PERIODICALLY-SYNCHRONOUS COUPLING OF ATMOSPHERE AND OCEAN MODELS

PART I: GENERAL STRATEGY AND APPLICATION  
TO THE CYCLO-STATIONARY CASE

by

ROBERT SAUSEN · REINHARD VOSS

HAMBURG, July 1995

AUTHORS:

Reinhard Voss

DKRZ  
Deutsches Klimarechenzentrum  
Bundesstraße 55  
D-20146 Hamburg  
Germany

Robert Sausen

Institut für Physik der Atmosphäre  
DLR Oberpfaffenhofen  
D-82234 Weßling  
Germany

MAX-PLANCK-INSTITUT  
FÜR METEOROLOGIE  
BUNDESSTRASSE 55  
D-20146 Hamburg  
F.R. GERMANY

Tel.: +49-(0)40-4 11 73-0  
Telefax: +49-(0)40-4 11 73-298  
E-Mail: <name> @ dkrz.d400.de



# Techniques for Asynchronous and Periodically-synchronous Coupling Of Atmosphere and Ocean Models

## Part I: General Strategy and Application To the Cyclo-stationary Case

R. Sausen<sup>1)</sup> and R. Voss<sup>2)</sup>

<sup>1)</sup> Institut für Physik der Atmosphäre, DLR Oberpfaffenhofen, D-82234 Weßling, Germany

<sup>2)</sup> Deutsches Klimarechenzentrum, Bundesstr. 55, D-20146 Hamburg, Germany

### Abstract

Asynchronous and periodically-synchronous schemes for coupling atmosphere and ocean models are presented. The performance of the schemes is tested by simulating the climatic response to a step function forcing and to a gradually increasing forcing with a simple zero-dimensional non-linear energy balance model. Both the initial transient response and the asymptotic approach of the equilibrium state are studied. If no annual cycle is allowed the asynchronous coupling technique proves to be a suitable tool. However, if the annual cycle is retained, the periodically-synchronous coupling technique reproduces the results of the synchronously coupled runs with smaller bias. In this case it is important that the total length of one synchronous period and one ocean only period is not a multiple of 6 months.

ISSN 0937-1060



# 1. Introduction

The most reliable results of numerical climate change studies are currently achieved using coupled atmosphere-ocean general circulation models (AOGCMs), which have been developed and applied by a variety of research groups (e.g. Washington and Meehl, 1989; Manabe et al., 1991; Cubasch et al., 1992; Lunkeit et al., 1995; Murphy, 1995). Unfortunately, these models are very consumptive in computer time. This restricts the simulation period to a few hundred years for low resolution models, like T21 or R15 (e.g. von Storch, 1994; Manabe and Stouffer, 1994), and to a corresponding shorter simulation period for models with higher resolution, for example T42.

As most of the computer resources during coupled AOGCM integrations are consumed by the atmospheric component, it appears necessary to explore a technique which reduces the computation time fraction of the atmospheric component. This could be achieved by simplifying the physical processes simulated by the atmosphere model, which would counteract the general tendency of improving models by implementing more sophisticated parameterizations. Another method is the application of asynchronous or periodically-synchronous coupling techniques. Here the simulated time periods for the atmosphere are shorter than for the ocean. Once such a fast integration technique is available, it would be possible, for instance, to extend the simulation period, to increase the model resolution or to perform a large number of simulations with different initial conditions in order to separate signal and noise (e.g. Cubasch et al., 1994).

In the asynchronous mode the atmospheric and the oceanic sub-models alternately run with stored boundary conditions which were previously computed by the respective other sub-model. This technique, applied with much shorter simulation periods for the atmosphere than for the ocean models, was used for models with annual mean forcing (e.g. Manabe and Bryan, 1969; Manabe and Stouffer, 1988) and for models including an seasonal cycle (e.g. Manabe et al. 1979, Washington et al., 1980).

The periodically-synchronous coupling scheme, which was suggested by Gates (Schlesinger, 1979), has been analysed by Schneider and Harvey (1986), Harvey (1986), Sausen(1988) and Roberts (1990) using energy balance models. This scheme consists of alternating synchronous (both sub-models are integrated quasi-simultaneously) and ocean only integrations with stored atmospheric conditions from the previous synchronous periods.

The objective of our investigation is the development of a computationally efficient coupling technique that is suitable for coupled AOGCMs including a seasonal cycle and the high internal variability of the atmosphere. The coupling technique should assure a coupled model integration with an output that is close to the results computed by the corresponding synchronously coupled model.

The development of asynchronous or periodically-synchronous coupling schemes requires a very large number of coupled atmosphere-ocean model integrations, more than can be afforded if AOGCMs were used. Therefore, we test these schemes with a simplified model which is easy to handle and very cheap in computer resources. Nevertheless, this model should include some main features which play an important role in the dynamics of coupled comprehensive models, i.e. time constants that vary over orders of magnitude, non-linearity, and a high quasi-stochastic variability as a substitute of the internal dynamical variability.

Sausen (1988) employed a simple three component energy balance model for testing asynchro-

nous coupling schemes. The non-linearity was included by a traditional formulation of the ice-albedo feedback (e.g. North et al., 1981). A high variability was introduced by an external stochastic forcing. Starting from this bases we have been able to refine coupling techniques and to test them rigorously by means of model runs. However, the most rigorous test is the application of a scheme, which has been selected as most suitable, to a more comprehensive AOGCM. Such a test is also provided.

However, in the current paper we concentrate on the general strategy of asynchronous and periodically-synchronous coupling and test various schemes by means of the simple model, either for the case with annual mean or annual cycle forcing. In a follow-up paper (Voss and Sausen, 1995) we will study the impact of stochastic variability and, finally, the application to an AOGCM will be described in a third paper (Voss et al., 1996).

In the following two sections the energy balance model and its behaviour in the synchronous mode are described. In order to gain insight into coupling problems asynchronously coupled experiments with annual mean forcing as well as periodically-synchronously coupled experiments with annual cycle forcing are conducted (Section 4). These experiments are run to simulate the response of the system to a step function forcing. In Section 5 the effect of a more realistic climate change scenario with a transient change in the forcing is investigated. The main conclusions follow in the final Section 6.

## 2. A simple atmosphere-ocean model

In order to investigate the mechanism of different coupling strategies, we make use of a zero-dimensional energy balance model which is an extension of the model used by Sausen (1988). If suitable designed, such a simple and computationally fast model exhibits some main features of the climate system. The model is non-linear due to its representation of the ice-albedo feedback. An annual cycle is introduced by an external forcing. The strongly different time scales of the atmosphere and the ocean are reflected in the choice of the model constants.

The following model equations express the heat balance of the atmosphere (1), the oceanic mixed layer (2), and the deep ocean (3):

$$C_A \frac{dT_A}{dt} = R_A - \lambda_A T_A + k_1 (T_{O1} - T_A) \quad (1)$$

$$C_{O1} \frac{dT_{O1}}{dt} = R_O - \lambda_O T_{O1} - k_1 (T_{O1} - T_A) + k_2 (T_{O2} - T_{O1}) \quad (2)$$

$$C_{O2} \frac{dT_{O2}}{dt} = -k_2 (T_{O2} - T_{O1}) \quad (3)$$

$C_A$ ,  $C_{O1}$  and  $C_{O2}$  denote the heat capacities of the atmosphere, the oceanic mixed layer, and the deep ocean, respectively.  $T_A$ ,  $T_{O1}$ , and  $T_{O2}$  are the temperatures of the respective sub-systems.  $k_1 (T_{O1} - T_A)$  and  $k_2 (T_{O2} - T_{O1})$  are the heat fluxes from ocean to atmosphere and from deep ocean to the oceanic mixed layer, respectively. In this paper the abbreviation  $F$  is used for the term  $k_1 (T_{O1} - T_A)$ , the flux coupling ocean and atmosphere.

The terms  $(R_A - \lambda_A T_A)$  and  $(R_O - \lambda_O T_{O1})$  represent the radiative forcing of atmosphere and ocean where the longwave radiation is linearized about a reference temperature. The terms  $R_A$  and  $R_O$  contain the solar forcing and the constant contribution by the longwave radiation of the atmosphere and the ocean, respectively.  $R_A$  consists of two parts, representing an annual mean forcing  $R_A^{(1)}$  and an annual cycle forcing  $R_A^{(2)} \sin(\omega t)$ :

$$R_A = R_A^{(1)} + R_A^{(2)} \sin(\omega t) \quad (4)$$

where  $\omega = 2\pi \text{ a}^{-1}$ .  $R_O$  comprises a parameterization of the ice-albedo feedback by a stepwise linear function (Figure 1). For oceanic mixed layer temperatures  $T_{O1}$  less than  $T_O^{(1)}$  the sea surface is completely ice-covered and  $R_O = R_O^{(1)}$ , while for temperatures greater than  $T_O^{(2)}$  the sea surface is ice-free and  $R_O = R_O^{(2)}$ . Between these two reference temperatures the forcing term  $R_O$  increases linearly with  $T_{O1}$  (5).

$$R_O(T_{O1}) = \begin{cases} R_O^{(1)} & \text{for } T_{O1} \leq T_O^{(1)} \\ R_O^{(1)} + \frac{T_{O1} - T_O^{(1)}}{T_O^{(2)} - T_O^{(1)}} \left( R_O^{(2)} - R_O^{(1)} \right) & \text{for } T_O^{(1)} < T_{O1} < T_O^{(2)} \\ R_O^{(2)} & \text{for } T_O^{(2)} \leq T_{O1} \end{cases} \quad (5)$$

Due to this traditional formulation of the non-linear ice-albedo feedback (e.g. North et al., 1981) the model has either one stable steady state solution, or two stable and one unstable solutions, depending on the choice of the parameters, if  $R_A = R_A^{(1)} = \text{constant}$  (Sausen and Lunkeit, 1990).



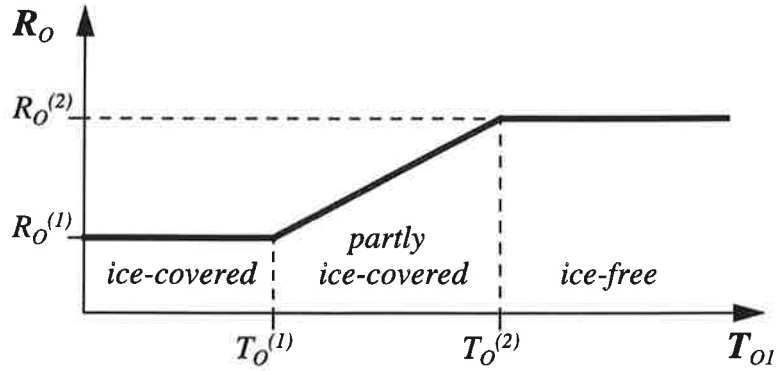


Figure 1: Scheme of the ice-albedo feedback.

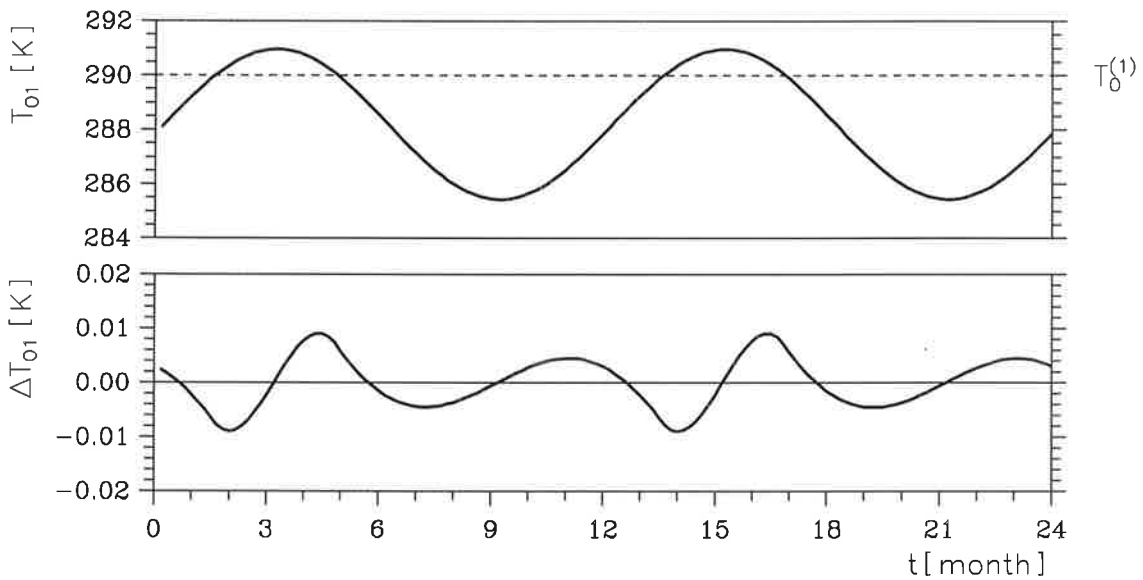


Figure 2: Two annual cycles of the oceanic mixed layer temperature  $T_{OI}$  (upper panel) and the difference between the annual cycle of this time series and the fitted first harmonic function of the annual cycle (bottom panel).

In the case of the cyclo-stationary forcing ( $R_A^{(2)} \neq 0$ ) the non-linearity of the model causes higher harmonics in the annual cycle of the model variables, despite the fact that the external forcing is sinusoidal (cf. (4)). Figure 2 shows the annual cycle of the oceanic mixed layer temperature  $T_{OI}$  for the constants of Table 1, and the differences between the annual cycle and the fitted first harmonic function. In this example the ocean is completely covered by ice ( $T_{OI} < T_O^{(1)} = 290$  K) for approximately 9 months a year. In relation to an amplitude of approximately 2.8 K the deviations from the sinusoidal annual cycle of at most 0.01 K are small. They would be larger, if the model was in the transition range between totally ice-covered and ice-free for a longer time.

The choice of the model constants (Table 1), especially the choice of the heat capacities and the coupling constants, results in different time constants for the uncoupled boxes. As is the case in the real climate system, the time constants of the atmosphere (10 days) and the oceanic mixed layer (110 days) are rather short compared to the constant of 160 years valid for the deep ocean. Since the relaxation time of the slowest sub-system mainly determines the relaxation time of the

complete coupled system the time constant of the deep ocean may be regarded as characteristic time of the coupled box model.<sup>1</sup>

Table 1: Standard values of the model constants.

	Atmosphere	Ocean
Heat capacity	$C_A = 10^7 \text{ Jm}^{-2}\text{K}^{-1}$	$C_{O1} = 10^8 \text{ Jm}^{-2}\text{K}^{-1}$ $C_{O2} = 10^9 \text{ Jm}^{-2}\text{K}^{-1}$
Solar input	$R_A^{(1)} = 130.0 \text{ Wm}^{-2}$ $R_A^{(2)} = 65.0 \text{ Wm}^{-2}$	$R_O^{(1)} = 120.0 \text{ Wm}^{-2}$ $R_O^{(2)} = 125.0 \text{ Wm}^{-2}$
Reference temperature		$T_O^{(1)} = 290.0 \text{ K}$ $T_O^{(2)} = 295.0 \text{ K}$
Emissivity	$\lambda_A = 0.5245 \text{ Wm}^{-2}\text{K}^{-1}$	$\lambda_O = 0.3472 \text{ Wm}^{-2}\text{K}^{-1}$
Coupling constant	$k_1 = 10.0 \text{ Wm}^{-2}\text{K}^{-1}$	$k_2 = 0.2 \text{ Wm}^{-2}\text{K}^{-1}$
Time step	$\Delta t_A = 0.5 \text{ d}$	$\Delta t_O = 5.0 \text{ d}$

---

<sup>1</sup> With 160 years the time constant of the model deep ocean underestimates the longest characteristic time of the real deep ocean. Nevertheless, we chose a shorter time in order to reduce the simulation period, which is necessary to come close to a new quasi-equilibrium, if the system is disturbed. For our purpose of testing coupling schemes, only the large differences in the time constant (several orders of magnitude) are important.

### 3. Synchronous coupling

Integrations of the synchronously coupled model are used as a reference in order to verify asynchronous and periodically-synchronous coupling techniques. In the synchronous mode the oceanic and the atmospheric sub-models are integrated quasi-simultaneously (Figure 3).

The atmospheric sub-model is integrated for a time period  $\tau$  ( $n_A$  atmosphere time steps) with boundary conditions given by the oceanic sub-model. Often, the temperature of the upper most ocean level and variables describing the sea-ice are transferred from the oceanic sub-model to the atmospheric sub-model, which then calculates the coupling fluxes (e.g. Cubasch et al., 1992; Lunkeit et al., 1995). In the case of our simple model, the oceanic mixed layer temperature  $T_{OI}$  is used by the atmospheric sub-model in order to calculate the heat flux  $F$  from the ocean to the atmosphere and the atmospheric temperature  $T_A$ . In a second step these coupling fluxes, averaged over the time period  $\tau$ , are taken as forcing for the integration of the oceanic sub-model over the same time period  $\tau$  ( $n_O$  ocean time steps). In the case of the box model the mean heat flux  $\bar{F}$  is transferred. The oceanic sub-model then calculates a new oceanic state, which is taken as boundary condition for the integration of the atmospheric sub-model over the next period  $\tau$ . A new integration cycle can then be started.

For the following simulations with the box model we have chosen  $\tau$  to be five days. This corresponds to ten time steps of the atmospheric part ( $n_A = 10$ ) and one time step of the oceanic part of the coupled model ( $n_O = 1$ ).

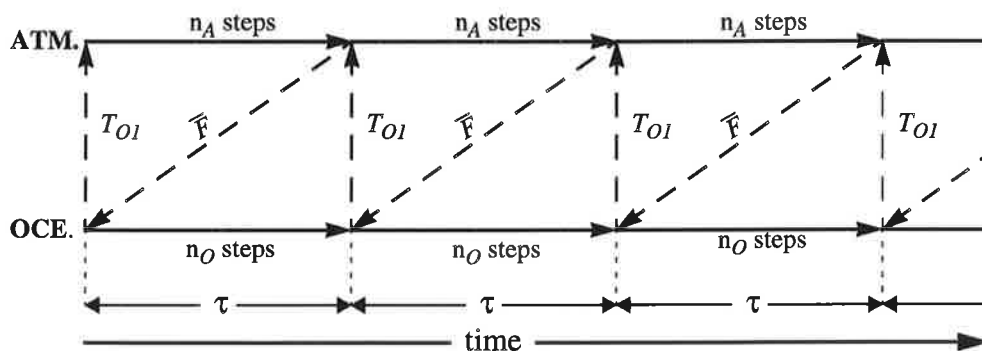


Figure 3: Synchronous coupling scheme.

The sensitivity of the model and the different coupling strategies are evaluated analysing the response to two different external forcings: a step function forcing and a forcing which first increases linearly with time and then after hundred years remains stationary. These two perturbations correspond, for instance, to a doubling  $\text{CO}_2$  experiment and to a transient  $\text{CO}_2$  experiment where the atmospheric  $\text{CO}_2$  content increases exponentially during the first hundred years (like the IPCC scenario A; Houghton et al., 1990).<sup>2</sup>

We have realized these perturbations by modifying the atmospheric emissivity (Figure 4). Firstly, an instantaneous reduction from the standard value  $\lambda_A$  to  $\lambda_{A(red)}$  at time  $t = 0$  is applied. Secondly, a linear reduction from  $\lambda_A$  to  $\lambda_{A(red)}$  between  $t = 0$  and  $t = 100$  a is assumed. For the following years the value of the atmospheric emissivity remains constant at  $\lambda_{A(red)}$ . In both sce-

<sup>2</sup> The radiative forcing is approximately a logarithmic function of the greenhouse gas concentration.

narios the final atmospheric emissivity  $\lambda_{A(red)} = 0.5144 \text{ Wm}^{-2}\text{K}^{-1}$  is 2 % lower than the standard value  $\lambda_A$  of Table 1. In the first case the model climate state will initially change rather rapidly, whereas a more gradual change is expected in the second case. The requirements on the quality of the coupling technique are higher in the first case than in the second one. On the other hand, the second case is the more realistic one with respect to possible scenarios of the greenhouse gas concentration.

In all following numerical experiments the energy balance model is integrated over 1000 years. Each experiment starts from the respective equilibrium state of the model version with the standard atmospheric emissivity  $\lambda_A$ . 1000 years are sufficient for the model in order to come close to its new equilibrium state. Results are plotted using a logarithmic time axes in order to display both, the initial (or transition) phase and the asymptotic approach of the equilibrium state, which is identical for both scenarios. The model version without annual cycle forcing ( $R_o^{(2)} = 0$ ) can be solved analytically. The reduction of the atmospheric emissivity results in an increase of the equilibrium temperature from  $T_{equ}$  to  $T_{equ(red)}$  (Table 2). The equilibrium temperatures increase by 9.08 K for the atmospheric box and by 9.26 K for both oceanic boxes. In the case of the instantaneous reduction of the atmospheric emissivity, the synchronously coupled model has already reached over 99 % of the expected equilibrium response after 1000 years integration time (see  $T_{ins}(1000a)$ ). For the simulation with linear reduction of the atmospheric emissivity the temperature increase after 1000 years (see  $T_{lin}(1000a)$ ) is more than 1 % smaller than in the other scenario..

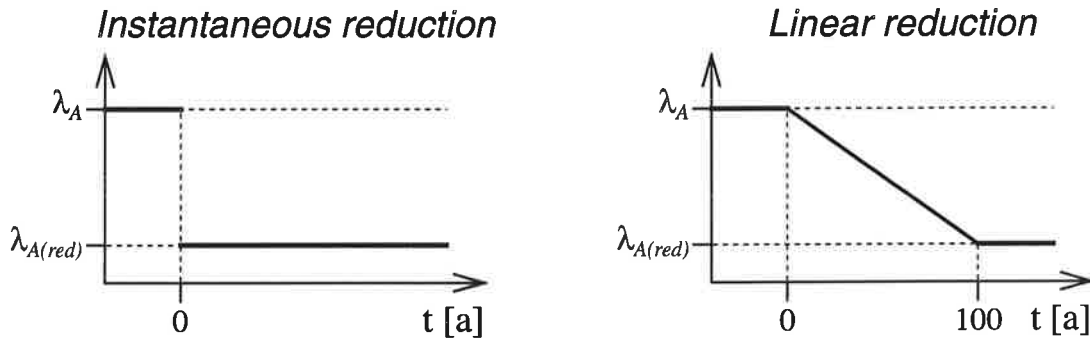


Figure 4: Temporal evolution of the atmospheric emissivity.

Table 2: Equilibrium temperatures [K] of the energy balance model with annual mean forcing for the standard atmospheric emissivity  $\lambda_A$  ( $T_{equ}$ ) and for the reduced value  $\lambda_{A(red)}$  ( $T_{equ(red)}$ ).  $T_{ins}(1000a)$  and  $T_{lin}(1000a)$  are simulated temperatures 1000 years after the instantaneous reduction of the emissivity and after the beginning of linear emissivity reduction, respectively.

	$T_{equ}$	$T_{equ(red)}$	$T_{ins}(1000a)$	$T_{lin}(1000a)$
Atmosphere	286.00	295.08	295.07	294.96
Oceanic mixed layer	288.00	297.26	297.25	297.13
Deep ocean	288.00	297.26	297.19	297.03

The transient response is much faster in the case with instantaneously reduced atmospheric emissivity than in the case with linear reduction (thick curves in Figure 5). Due to its much longer time constant the deep ocean exhibits a delayed response in both experiments, whereas the atmosphere and the oceanic mixed layer behave rather similar as consequence of the strong coupling.

If the annual cycle of the solar forcing is included ( $R_O^{(2)} \neq 0$ , thin curves in Figure 5), the response is initially larger than in the case without annual cycle of the solar forcing. But after a while the curves cross over and converge more slowly to the new quasi-equilibrium than in the experiment without annual cycle.

As long as the temperature of the oceanic mixed layer  $T_{OI}$  does not pass one of the critical temperatures  $T_O^{(1)}$  or  $T_O^{(2)}$ , the model can be treated as if it was linear. However, if the annual cycle is included,  $T_{OI}$  changes during the annual cycle the three domains defined by equation (5), and the non-linearity of the model can be noticed: the annual means of the equilibrium temperatures are different from those obtained without the annual cycle of the solar forcing. If the annual cycle is included the equilibrium annual mean temperatures of all three boxes for the case with atmospheric emissivity  $\lambda_A$  are approximately 0.2 K higher than with annual mean forcing only ( $T_{equ}$  in Table 2).

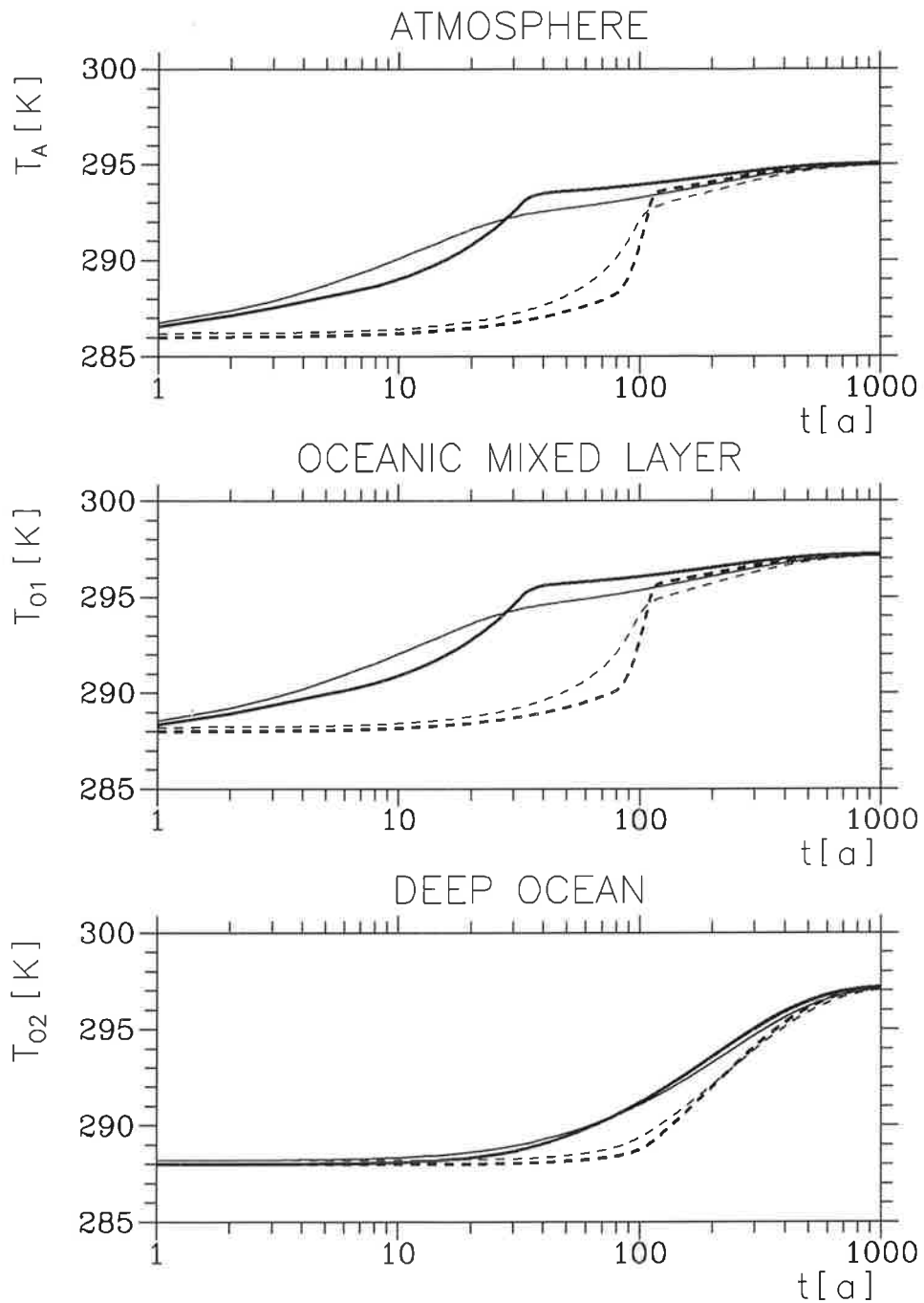


*Figure 5:* Time evolution of the annual mean temperature of synchronously coupled experiments with (thin curves) and without (thick curves) annual cycle of the atmospheric forcing for the instantaneous (solid curves) and the linear reduction (dashed curves) of the atmospheric emissivity.

## 4. Asynchronous and periodically-synchronous coupling schemes and their applicability in the case of step function forcing

### 4.1 Tests without annual cycle of the solar forcing

Beginning in the late sixties several asynchronous coupling techniques have been applied. Manabe and Bryan (1969), for example, carried out a simulation with an asynchronously coupled model where only the annual mean insolation was considered. In this run 3 hours of atmospheric model integration were followed by 12.5 days of the oceanic model.

This asynchronous coupling scheme was adapted to our simple model for the case without the annual cycle of the solar forcing ( $R_o^{(2)} = 0$ ). Figure 6 displays the scheme. At the beginning of the loop the oceanic mixed layer temperature  $T_{O1}$  is given to the atmospheric sub-model where it serves as fixed boundary condition for the integration over a period  $\tau_A$ . During the last five days of this integration period the air-sea heat flux  $F$  is averaged. After the  $n_A$  atmosphere time steps are finished the averaged flux  $\bar{F}$  is taken as forcing for the oceanic sub-model during the period  $\tau_O$  ( $n_O$  time steps). A new  $T_{O1}$  is provided at the end of this period for the following integration of the atmospheric sub-model.

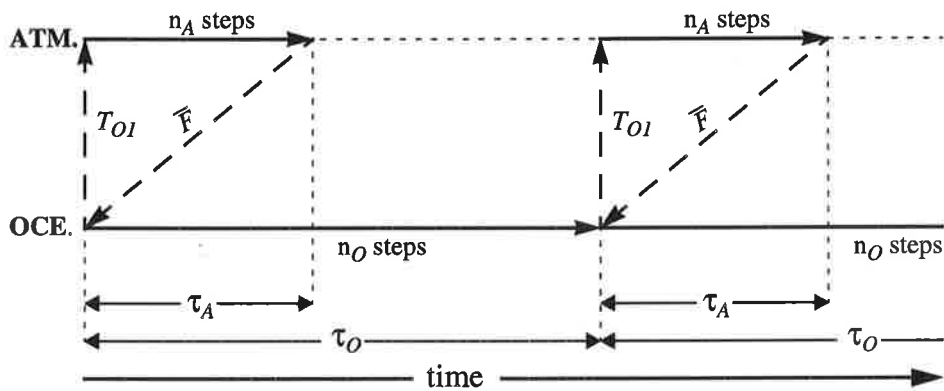
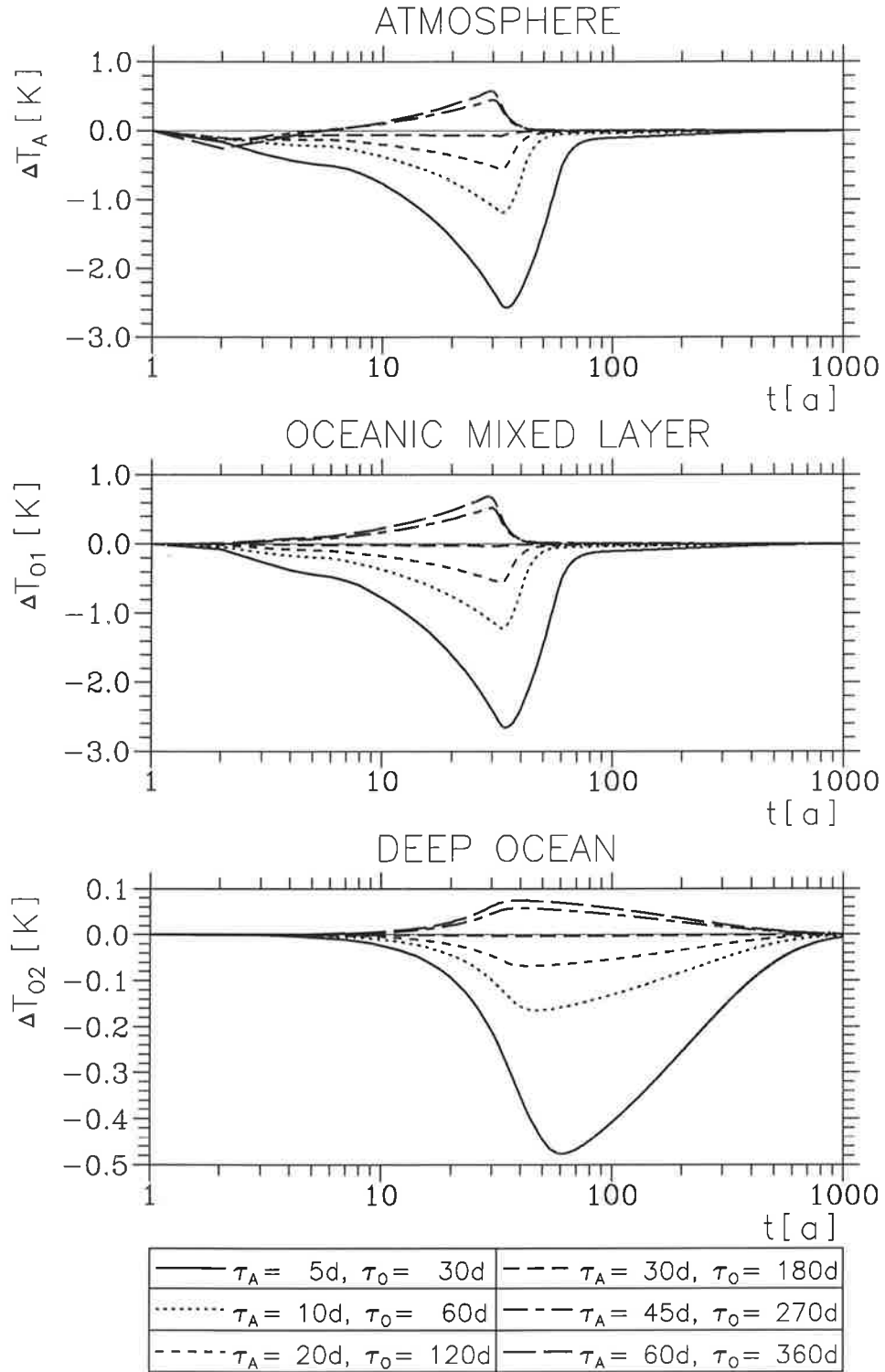


Figure 6: Asynchronous coupling scheme.

If  $\tau_O = \tau_A$ , the scheme was identical to the synchronous coupling scheme (cf. Figure 3). However, in order to be economic,  $\tau_O$  should be much larger than  $\tau_A$ . Manabe and Bryan (1969) chose the ratio  $\tau_A : \tau_O = 1 : 100$ , a value which appears to us as too small, in view of our own climate change experiments. For our experiments a ratio of  $1 : 6$  was chosen. Six experiments were performed with  $\tau_A = 5, 10, 20, 30, 45$  and  $60$  days and the corresponding ocean periods  $\tau_O$  six times as long. The computational expense of all experiments is identical. In order to test the asynchronously coupled model versions the atmospheric emissivity is instantaneously reduced at  $t = 0$ .

Figure 7 shows the temperature errors relative to the synchronous reference simulation (solid thick curves in Figure 5). All asynchronously coupled experiments exhibit differences in the transient response compared to the synchronously coupled reference run, but all finally converge to the new state of the synchronously coupled reference run. The temperature errors of the atmosphere and the oceanic mixed layer are of a similar magnitude, whereas the errors of the deep ocean are much smaller and reduce less rapidly. Both, an overshooting ( $\tau_A = 45, 60$  d)



*Figure 7:* Differences of the annual mean temperature between the synchronously coupled reference experiment and asynchronously coupled experiments with annual mean forcing and different length of the integration periods  $\tau_A$  and  $\tau_O$ . All experiments are performed with instantaneously reduced atmospheric emissivity.



and an underestimation ( $\tau_A = 5, 10, 20, 30$  d) of the “true” synchronous response can be observed. In the case of short  $\tau_A$  the underestimation is caused by a phase error of the system: the asynchronously coupled system reacts too late. With increasing atmospheric integration period  $\tau_A$  a second error with opposite sign becomes more important: the atmosphere initially stays too cold (cf. Figure 7 top panel). The result is too large an ocean-atmosphere heat flux  $F$  which then is kept constant for a rather long period. Due to the effect of two compensating errors with different growth rates as function of  $\tau_A$ , the total error will be minimal for some  $\tau_A$ . The most successful realisation with the smallest temperature errors of the presented experiments is the simulation with  $\tau_A = 30$  days and  $\tau_O = 180$  days. The maximum differences are less than 1 % of the expected temperature response of more than 9 K (see Section 3).

In the synchronous mode the heat flux into the ocean changes every ocean time step, while in the ocean only periods of the asynchronous integration the flux is kept constant for a rather long period. This effect could be reduced by applying an extrapolation procedure. If a linear or quadratic extrapolation of the heat flux during the ocean integrations is applied, the effects in the transient behaviour are, however, much smaller than changes in the error caused by variations in the length of the integration periods. Two features are mainly responsible for this behaviour. Firstly, errors occur due to the rare exchange of information between both sub-models, if the integration periods are too long, especially  $\tau_O$ . Secondly, the conditions of the initial adjustment of the atmospheric sub-model after the ocean integration are allowed to influence the oceanic integration if  $\tau_A$  is too short. Therefore, the optimal length of the integration periods depends on the relaxation time of the sub-systems.

## 4.2 Tests with annual cycle

The asynchronous coupling technique, which was described in the Section 4.1, can not be successfully applied to coupled models including an annual cycle. The demand for an accurate representation of an annual cycle in addition to the necessity of a frequent exchange of information between both sub-models causes problems. Nevertheless further developments of this technique, which are also applied to models including an annual cycle, exist (e.g. Manabe et al., 1979; Washington, 1980).

Another more promising method, suggested by Gates, is referred to as “periodically-synchronous coupling” (Schlesinger, 1979). This method is a combination of synchronous coupling and ocean only integrations (Figure 8). During the synchronous periods the atmospheric and the oceanic sub-models are integrated quasi-simultaneously over a time period  $\tau_{syn}$  (cf. Section 3). In the other mode only the oceanic sub-model is integrated over a time period  $\tau_{oce}$  with boundary conditions taken from a data bank. This data bank contains at least one annual cycle of the forcing for the ocean calculated by the atmospheric sub-model during the synchronous periods. In our case the 5-days-means of the heat flux  $F$  are stored in the data bank.

All presented tests of the periodically-synchronous coupling technique start with a synchronous period  $\tau_{syn}$  of 24 months. The starting point coincides with the beginning of the atmospheric emissivity reduction. The following synchronous periods last 15 months from which only the last 12 months are used to update the data bank.

The time evolution of the heat flux  $F$ , the atmospheric temperature  $T_A$  and the oceanic mixed layer temperature  $T_{O1}$  for a periodically-synchronously coupled run with  $\tau_{oce} = 66$  months is shown in Figure 9. This choice of the period length results in a ratio  $\tau_{syn} : \tau_{oce}$  of 1 : 4.4. The fitted first harmonic function, which contains the main part of the annual cycle is subtracted in

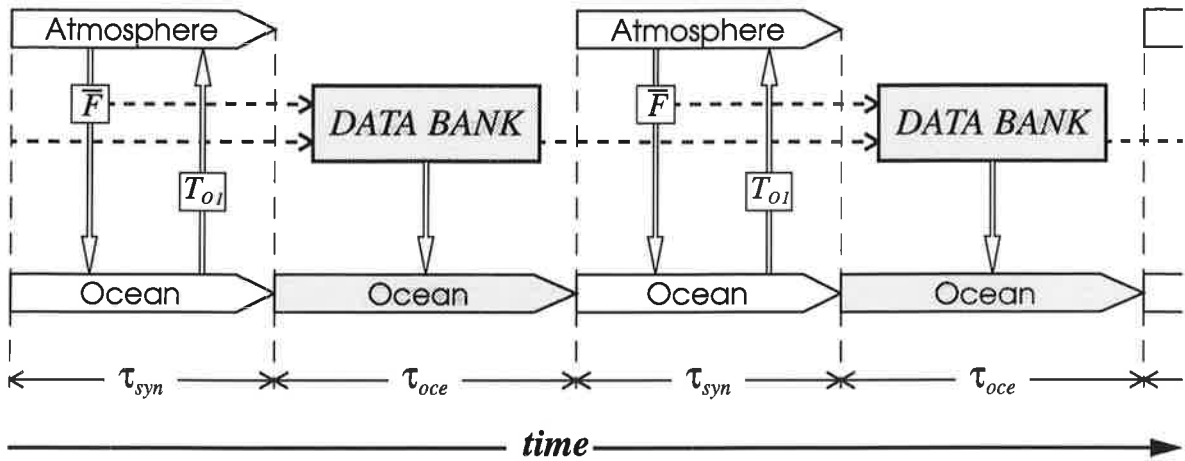


Figure 8: Periodically-synchronous coupling scheme.

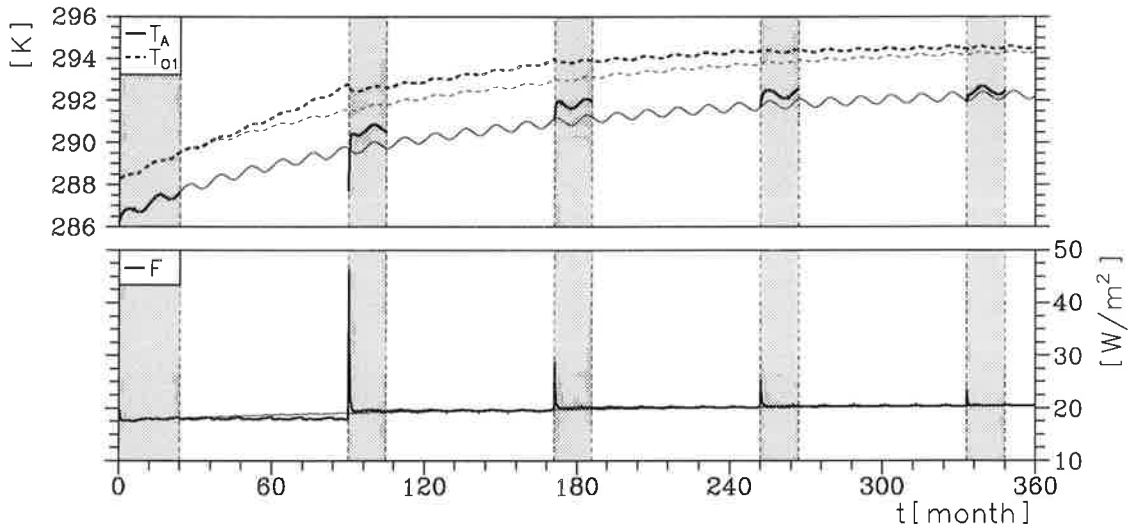
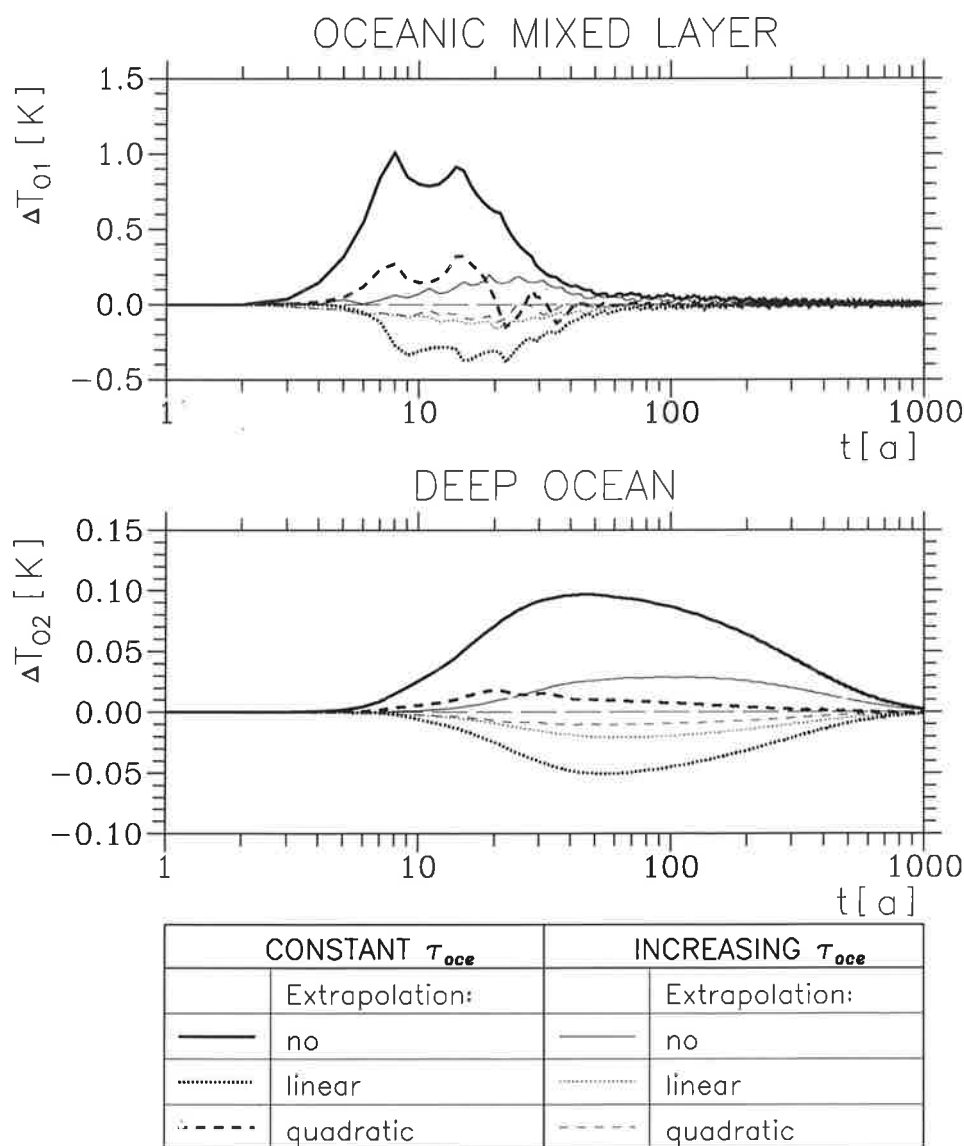


Figure 9: Time evolution of the first 30 years of a periodically-synchronously coupled run with constant length of the ocean only periods  $\tau_{oce}$  and instantaneously reduced atmospheric emissivity (thick curves). The synchronous periods are shaded. The corresponding fitted first harmonic function is subtracted from all curves. The thin curves indicate the evolution of the synchronous reference run.

order to emphasize the signals on larger time scales. The remaining oscillations are caused by the non-linearity of the model (see Section 2). In this example the annual cycle of  $F$  calculated during the last synchronously coupled year is taken as forcing for the following ocean only period. Due to the instantaneous reduction of the atmospheric emissivity at time  $t = 0$  the temperatures  $T_A$  and  $T_{OI}$  increase continuously during the first synchronous period. The increase of  $T_{OI}$  continues during the following ocean only integration period. Due to an underestimated heat flux relative to the synchronous case the warming of the oceanic mixed layer is overestimated. Since the state of the atmosphere has not changed during the integration of the ocean, the atmosphere must adjust to the new boundary conditions (approx. 3 K higher  $T_{OI}$  after the first ocean only integration) at the beginning of the following synchronous period. This happens by

an abrupt increase of the heat flux from ocean to atmosphere. As a consequence the atmosphere rapidly warms whereas the ocean cools, but both boxes remain more than 0.5 K too warm. During the following integration the errors decrease. In order to avoid that this atmospheric adjustment process at the beginning of a synchronous period enters into the forcing of the next ocean only integration period only the heat fluxes of the last 12 months of a synchronous period, which in total lasts 15 months, are stored in the data bank. Due to a smaller change of the oceanic state the shock at the beginning of the synchronous periods decreases as the simulation time proceeds.

The previously shown discrepancies in the transient climate response also occur in the time evolution of the annual mean temperatures. Figure 10 compares the annual mean temperatures of the periodically-synchronously coupled run (thick solid curves) with the synchronously coupled reference run (thin solid curves in Figure 5). As the annual mean values of  $T_A$  and  $T_{OI}$  behave similarly, the results of the atmospheric box are not shown. The largest differences in the upper



*Figure 10:* Differences of the annual mean ocean temperatures between periodically-synchronously coupled experiments and the synchronously coupled reference experiment. All experiments are performed with instantaneously reduced atmospheric emissivity.

ocean temperature occur during the first decades and decrease rapidly during the next decades to errors of less than 0.1 K. During the following centuries the remaining error decreases more slowly. The differences of the deep ocean are nearly an order of magnitude smaller, the maximum occurs later and the discrepancies are extended over the rest of the simulation.

The transient behaviour can substantially be improved by using an extrapolation scheme for the determination of the heat fluxes during the ocean only periods. The extrapolation is based on a linear or quadratic fit to the monthly mean flux of the last month of the just finished synchronous period and the corresponding month in the annual cycle of the previous synchronous periods (one previous period is used for the linear extrapolation, and two previous periods for the quadratic extrapolation). In order to obtain an annual cycle of the forcing, which represents the state at the end of the current synchronous period, the linear trend during this synchronous period is corrected for each value of the annual cycle. A linear and a quadratic extrapolation of this corrected annual cycle set is taken as forcing for the ocean only integrations. Whereas the run with linear extrapolation tends to underestimate the transient temperature response of the synchronously coupled model, the results with quadratic extrapolation exhibit a slight overestimation (thick dotted and dashed curves in Figure 10). Nevertheless, the transient behaviour of the simulations with extrapolation, especially with quadratic extrapolation, is substantially improved.

An additional improvement can be achieved, if a scheme with increasing length of  $\tau_{oce}$ , which was successfully applied by Schneider and Harvey (1986), is used. In the following examples  $\tau_{oce}$  is chosen to be subsequently 6, 12, 18, 24, 30, 39, 48, 57 months, and finally 66 months for the rest of the simulation. In other words, the synchronous mode of the coupled model is more frequently used in the first 30 years of the simulation time. Due to the shortening of periods without integration of the atmospheric sub-model the initial shock at the beginning of the synchronous periods is smaller and remains at the same level with increasing length of  $\tau_{oce}$ . This is illustrated by Figure 11 for the case without extrapolation. After about 10 years a period with temperatures  $T_A$  and  $T_{O1}$  slightly higher than in the synchronous case starts.

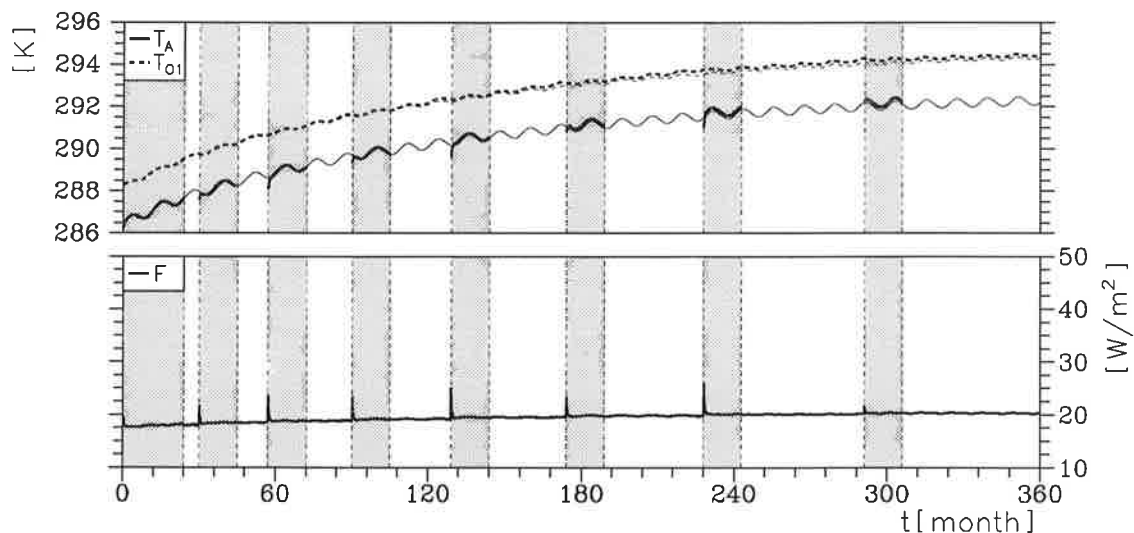


Figure 11: Time evolution of the first 30 years of a periodically-synchronously coupled run with increasing length of the ocean only periods  $\tau_{oce}$  and instantaneously reduced atmospheric emissivity (thick curves). The synchronous periods are shaded. The corresponding fitted first harmonic function is subtracted from all curves. The thin curves indicate the evolution of the synchronous reference run.

The time evolution of the annual mean temperatures also exhibits an improvement in all three cases, without, with linear and with quadratic extrapolation (thin curves in Figure 10), relative to the respective runs with ocean only periods of constant length. As in the experiments with constant  $\tau_{oce}$  extrapolation reduces the temperature error. Both experiments with extrapolation underestimate the temperature response, but in comparison to the experiments with constant  $\tau_{oce}$  the maximum error is nearly halved to less than 0.2 K for  $T_{OJ}$ .

### 4.3 The impact of the ocean only period length

So far the length of the ocean only periods  $\tau_{oce}$  was constant (66 months), apart from some experiments with smaller values at the beginning of the simulation. Here we analyse the impact of the length of the period  $\tau_{oce}$  on the performance of the procedure by means of the root mean square (rms) error of the annual mean oceanic mixed layer temperature. Only examples of the periodically-synchronous coupled model with annual cycle forcing are shown. The runs are performed using different, but for each run constant, values of  $\tau_{oce}$ . In accordance with the previously shown experiments the first synchronous period lasts 24 months and all following synchronous periods last 15 months.

As shown in Section 4.2 the strongest response of the coupled model and the largest discrepancies in the transient behaviour of the various model versions occur immediately after the instantaneous reduction of the atmospheric emissivity. Therefore, the rms errors of the first 200 years are of special interest (Figure 12a). With increasing  $\tau_{oce}$  the rms error of this period also increases, as one might expect, and therefore, the quality of the results produced by the periodically-synchronously coupled model decreases. In accordance with the results presented earlier, the error decreases if a linear or quadratic extrapolation scheme is applied.

The last 200 simulated years are another interval of particular interest. This interval is characterized by a system already rather close to its new quasi-equilibrium. Hence, the rms error of this period can be used as a measure for the asymptotic behaviour of the coupling scheme. Much smaller simulation errors can be expected. The rms error exhibits periodically pronounced maxima (Figure 12b). Regardless whether an extrapolation scheme is used or not maxima of the rms error occur every 12 months beginning with  $\tau_{oce} = 9$  months (i.e.,  $\tau_{oce} + \tau_{syn} = 24$  months) and with decreasing amplitude for increasing period length  $\tau_{oce}$ . A series of secondary maxima occurs shifted a half period of the annual cycle with increasing amplitude for increasing  $\tau_{oce}$ , especially for the series of experiments with linear extrapolation. In other words, the largest errors occur when the synchronous periods start at the same point of the annual cycle every (decreasing maxima) or every second time (increasing maxima). On the other hand, the values of the minima of the error remain at the same level of about 0.006 K. Hence, it is practicable to extend  $\tau_{oce}$  in the last 200 years of the simulation from less than one year to more than seven years without a reduction of quality in the model results, provided that  $\tau_{oce} + \tau_{syn}$  is not too close to a multiple of 6 months. The case with  $\tau_{oce} = 66$  months, which was previously used, fulfils this criterion.

Results computed for different length of  $\tau_{syn}$  and the corresponding rms errors of the deep ocean temperature show the same features. For  $\tau_{oce}$  longer than 96 month (not shown) the error of the model version with linear extrapolation increases drastically not only in the interval from 801-1000, but also during the first 200 simulated years.

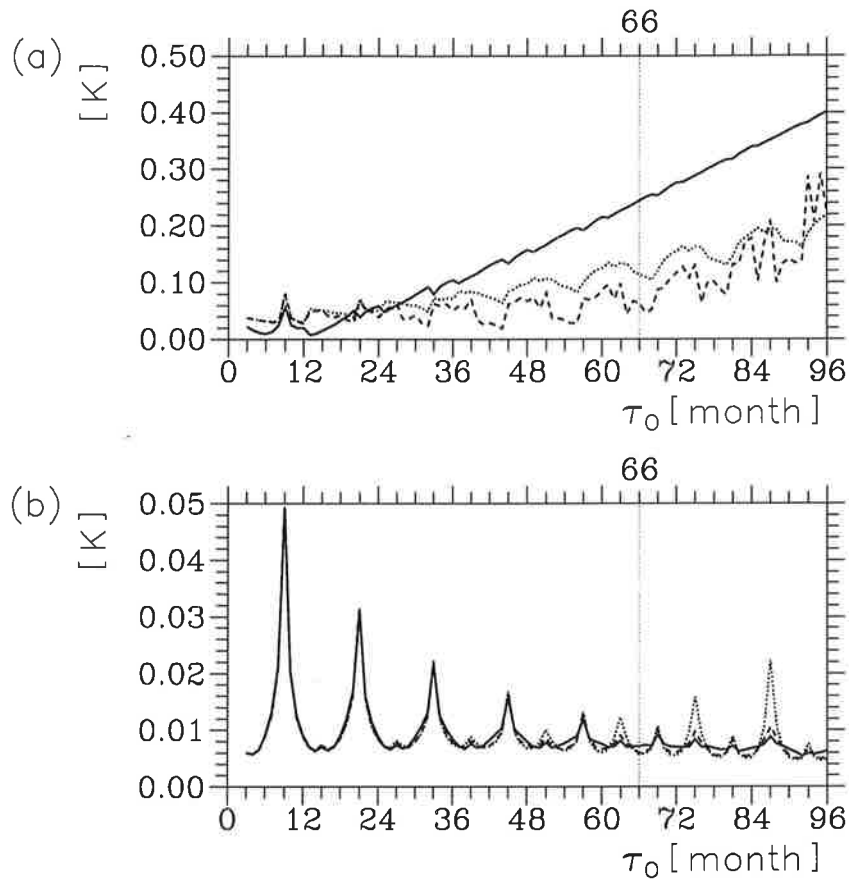


**Figure 12:** Rms errors of the annual mean oceanic mixed layer temperature  $T_{OI}$  for the year 1-200 (a) and 801-1000 (b). The curves represent rms errors of experiments without (solid) with linear (dotted) and with quadratic extrapolation (dashed) as function of the ocean only period length  $\tau_{oce}$ .

## 5. The application of the periodically-synchronous coupling scheme to experiments with linear emissivity reduction

An important application of coupled atmosphere-ocean models is the performance of transient climate change experiments like scenarios with prescribed time-dependent  $\text{CO}_2$  increase. In such experiments the forcing gradually increases. A response experiment of this kind should be more easily treated with our coupling scheme. In the following, we describe how such a gradually increasing forcing affects the fidelity of the periodically-synchronously coupled model.

In addition to the experiments with instantaneously reduced atmospheric emissivity, a series of experiments with a linear reduction of the emissivity during the first hundred years of the simulation was performed (cf. Section 3). In Figure 13 the first 30 years of an integration with constant ocean only integration periods  $\tau_{oce}$  of 66 months are shown. Compared to the case with instantaneously reduced  $\lambda_A$  (Figure 9) the response during the first 30 years is weaker. Therefore, the changes in the state of the ocean during the ocean only integrations and the resulting shock of the atmospheric sub-model at the beginning of the synchronous periods, due to changed boundary conditions, is drastically reduced (compare with Figure 9). This observation suggests that in this case it is not necessary to apply the method with increasing length of  $\tau_{oce}$ .

The above finding is emphasized by the comparison of the time evolution of the annual mean temperatures. Figure 14 compares the temperature error of experiments with and without increasing  $\tau_{oce}$ . In contrast to the simulations with step function forcing the introduction of the increasing period length does not have much impact on the transient behaviour.

The application of an extrapolation scheme, on the other hand, also reduces the errors in the case with time-dependent forcing. The comparison of the temperature errors (Figures 10 and 14) indicates that the transient behaviour is generally better reproduced in the experiments with time-dependent emissivity reduction. The maximum errors are nearly an order of magnitude smaller (note the different scaling of the temperature axes of Figures 10 and 14).

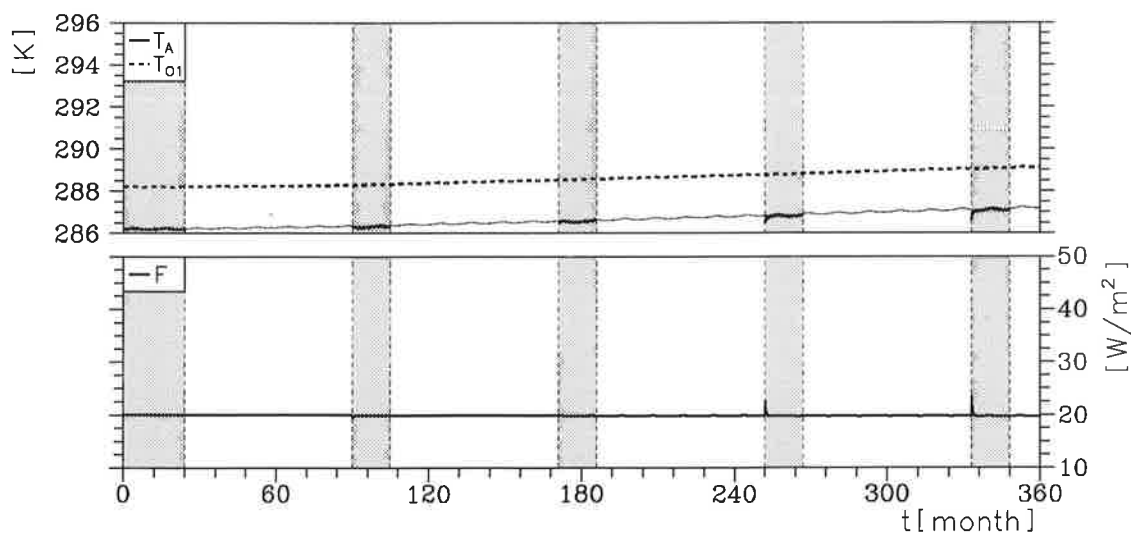


Figure 13: Time evolution of the first 30 years of a periodically-synchronously coupled run with constant length of the ocean only periods  $\tau_{oce}$  and linear reduction of the atmospheric emissivity (thick curves). The synchronous periods are shaded. The corresponding fitted first harmonic function is subtracted from all curves. The thin curves indicate the evolution of the synchronous reference run.

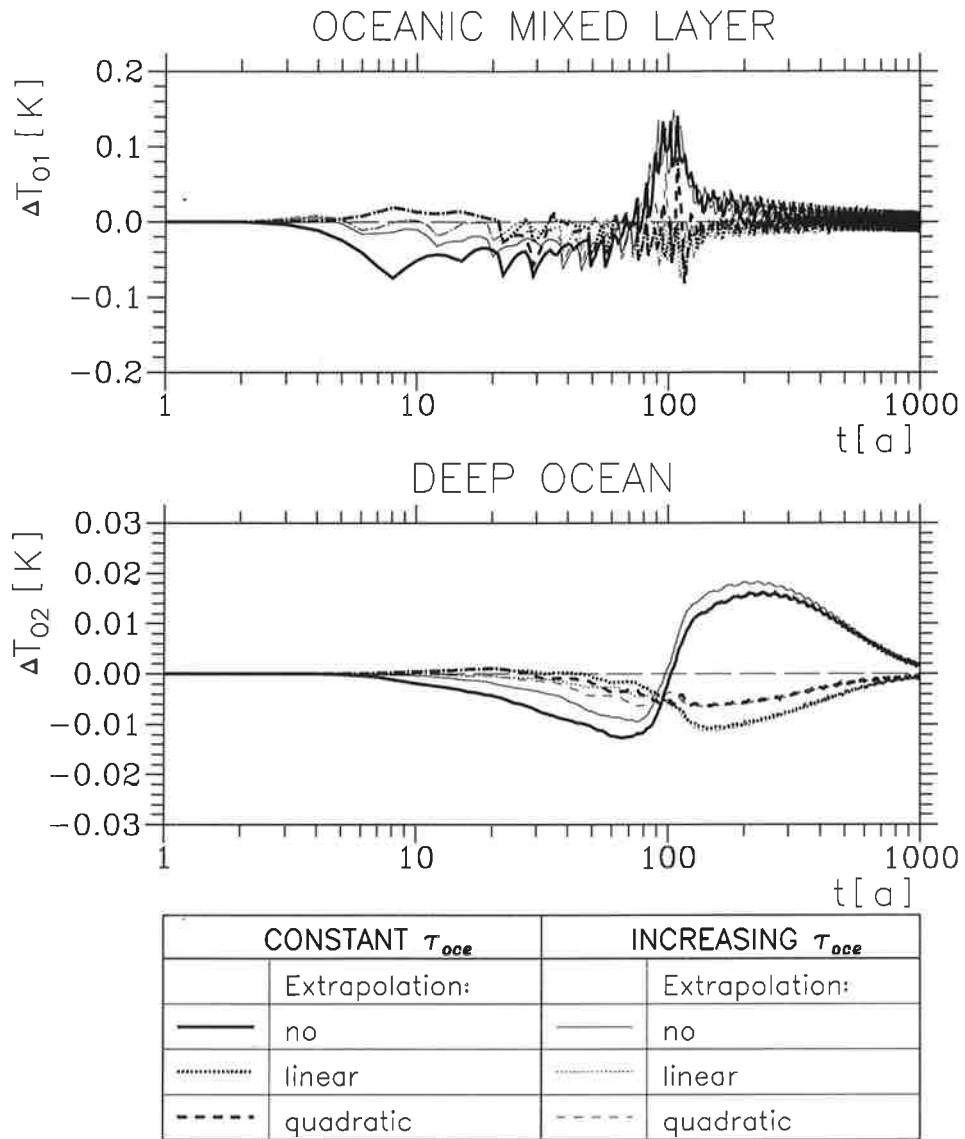


Figure 14: Differences of the annual mean ocean temperatures between periodically-synchronously coupled experiments and the synchronously coupled reference experiment. All experiments are performed with linear reduction of the atmospheric emissivity.



## 6. Conclusions

Asynchronous and periodically-synchronous schemes for coupling atmosphere and ocean models have been presented. By means of a zero-dimensional non-linear energy balance model of ocean and atmosphere, the responses of the asynchronously and periodically-synchronously coupled models to a step function decrease and to a gradual decrease of the atmospheric emissivity were investigated. The results have been compared to the corresponding synchronously coupled experiments.

The asynchronous coupling scheme, which was only applied to the model with annual mean forcing, exhibits a strong sensitivity to changes in the length of the integration periods. The application of an extrapolation scheme has only a minor effect. The behaviour of the asynchronously coupled model is mainly controlled by the adjustment time of the sub-models and the interval of information exchange between the sub-models.

The periodically-synchronous coupling method was applied to the model version with annual cycle forcing. The transient behaviour of the periodically-synchronous coupled model can be improved using an extrapolation scheme for the determination of the forcing during the ocean only periods. In the case of an instantaneous reduction of the atmospheric emissivity an additional improvement can be obtained by applying a method with increasing length of the ocean only integration periods. With this coupling scheme the transient behaviour of the corresponding synchronously coupled model is reasonably well reproduced. Tests with different length of the ocean only integration periods show an increasing error with increasing period lengths during the first 200 simulated years which are characterized by a strong climate change signal. Considering the years 801-1000, a period with a model state close to an equilibrium, maxima of the rms error occur periodically, if the cycle of the synchronous and the ocean only integration periods starts at the same point of the annual cycle every or every second time.

Choosing a more realistic scenario with a linear reduction of the atmospheric emissivity during the first hundred years of the simulation, the errors in the transient behaviour are nearly an order of magnitude smaller than in the case with step function forcing. The application of the method with increasing length of the ocean only integration periods has only minor effects and is therefore not necessary.

So far the periodically-synchronous coupling technique poses to be a rather promising tool for reducing the computational resources needed for long atmosphere-ocean simulations. However, an important aspect of comprehensive coupled atmosphere-ocean models has not been considered: the internal variability beyond the annual cycle. Our simple model was not able to reproduce this feature. This variability affects the determination of the forcing of the oceanic sub-model during the ocean only integrations. In Part II (Voss and Sausen, 1995) we will investigate the problems arising from the variability in detail.

### Acknowledgments:

The work was supported by grants from the climatic program of the European Union (EPOC-0003-C(MB) and EV5V-CT92-0123). The authors would like to thank Mr. Kristof Richmond for his advice concerning the English language.

## References:

- Cubasch, U., K. Hasselmann, H. Höck, E. Maier-Reimer, U. Mikolajewicz, B.D. Santer and R. Sausen, 1992: Time-dependent greenhouse warming computations with a coupled ocean-atmosphere model. *Clim. Dyn.*, 8, 55-69.
- Cubasch, U., B.D. Santer, A. Hellbach, G. Hegerl, H. Höck, E. Maier-Reimer, U. Mikolajewicz, A. Stössel and R. Voss, 1994: Monte Carlo climate change forecasts with a global coupled ocean-atmosphere model. *Clim. Dyn.*, 10, 1-19.
- Harvey, L.D.D., 1986: Computational efficiency and accuracy of methods for asynchronously coupling atmosphere-ocean models. Part II: Testing with a seasonal cycle. *J. Phys. Oceanogr.*, 16, 11-24.
- Houghton, J.T., G.J. Jenkins and J.J. Ephraums, (eds), 1990: Climate change: The IPCC scientific assessment. *Cambridge University Press, Cambridge*, 363 pp.
- Lunkeit, F., R. Sausen and J.M. Oberhuber, 1995: Climate simulations with the global coupled atmosphere-ocean model ECHAM2/OPYC. Part I: Present-day climate and ENSO events. *Submitted to Clim. Dyn.*
- Manabe, S., and K. Bryan, 1969: Climate calculations with a combined ocean-atmosphere model. *J. Atm. Sci.* 26, 786-789.
- Manabe, S., K. Bryan and M.J. Spelman, 1979: A global ocean atmosphere climate model with seasonal variation for future studies of the climate system. *Dyn. Atmos. Oceans*, 3, 393-426.
- Manabe, S., and R.J. Stouffer, 1988: Two stable equilibria of a coupled ocean-atmosphere model. *J. Clim.*, 1, 841-866.
- Manabe, S., R.J. Stouffer, M.J. Spelman and K. Bryan, 1991: Transient response of a coupled ocean-atmosphere model to gradual changes of atmospheric CO<sub>2</sub>. Part I: Annual mean response. *J. Clim.*, 4, 785-818.
- Manabe, S., and R.J. Stouffer, 1994: Multiple-century response of a coupled ocean-atmosphere model to an increase of the atmospheric carbon dioxide. *J. Clim.*, 7, 5-23.
- Murphy, J.M., 1995: Transient response of the Hadley centre coupled ocean-atmosphere model to increasing carbon dioxide. Part I: Control climate and flux adjustment. *J. Clim.*, 8, 36-56.
- North, G.R., R.F. Cahalan and J.A. Coakley, 1981: Energy balance climate models. *Rev. Geoph. Space Phys.*, 19, 91-121.
- Roberts, D.L., 1990: An investigation of the Gates asynchronous coupling strategy using a simple energy-balance model. *Dyn. Atmos. Oceans*, 14, 279-301.
- Sausen, R., 1988: Asynchronous coupling of ocean and atmosphere models. In: *Modelling the Sensitivity and Variations of the Ocean-Atmosphere System*. Report of a workshop at the ECMWF. WCRP-15, WMO/TD-No. 254, 280-289.
- Sausen, R., and F. Lunkeit, 1990: Some remarks on the cause of the climate drift of coupled ocean-atmosphere models. *Beitr. Phys. Atmosph.*, 63, 141-146.
- Schlesinger, M.E., 1979: Discussion of "A global ocean-atmosphere model with seasonal variation for future studies of climate sensitivity". *Dyn. Atmos. Oceans*, 3, 427-432.

- Schneider, S.H., and L.D.D. Harvey, 1986: Computational efficiency and accuracy of methods for asynchronously coupling atmosphere-ocean models. Part I: Testing with a mean annual model. *J. Phys. Oceanogr.*, 16, 3-10.
- von Storch, J.-S., 1994: Interdecadal variability in a global coupled model. *Tellus*, 46A, 419-432.
- Voss, R., and R. Sausen, 1995: Techniques for asynchronous and periodically-synchronous coupling of atmosphere and ocean models. Part II: The impact of the variability. *In preparation*.
- Voss, R., R. Sausen and U. Cubasch, 1996: Periodically-synchronously coupled integrations with the atmosphere-ocean general circulation model ECHAM3/LSG. *In preparation*.
- Washington, W.M., A.J. Semtner, G.A. Meehl, D.J. Knight and T.A. Mayer, 1980: A general circulation experiment with a coupled atmosphere, ocean and sea ice model. *J. Phys. Oceanogr.*, 10, 1887-1908.
- Washington, W.M., and G.A. Meehl, 1989: Climate sensitivity due to increased CO<sub>2</sub>: Experiments with a coupled atmosphere and ocean general circulation model. *Clim. Dyn.*, 4, 1-38.